Groundwater Research Report
WR16R006

# Effect of geochemical conditions on radium mobility in discrete intervals within the Midwestern Cambrian-Ordovician aquifer system

Madeleine Mathews
Madeline Gotkowitz
Matthew Ginder-Vogel

2019

Project number WR16R006

# Effect of geochemical conditions on radium mobility in discrete intervals within the Midwestern Cambrian-Ordovician aquifer system

**Madeleine Mathews**
Environmental Chemistry and Technology, Department of Civil and Environmental Engineering, University of Wisconsin – Madison, Madison, WI

**Madeline Gotkowitz**
Wisconsin Geological and Natural History Survey, Madison, WI
Current Affiliation: Montana Bureau of Mines and Geology, Butte, MT

**Matthew Ginder-Vogel**
Environmental Chemistry and Technology, Department of Civil and Environmental Engineering, University of Wisconsin – Madison, Madison, WI

Administered by:
University of Wisconsin Water Resources Institute

Funded by:
The National Institutes for Water Resources, U.S. Geological Survey 104b program
State of Wisconsin Groundwater Research and Monitoring Program

2019

*This project was supported by the United States Geological Survey National Institutes for Water Resources 104b program. Under the provisions of section 104 of the Water Resources Research Act of 1984, annual base grants (104b) are awarded to the Institutes or Centers that have been established in each of the 50 states, the District of Columbia, Puerto Rico, the U.S. Virgin Islands, and Guam. The annual base grants help each Institute or Center to plan and conduct applied and peer reviewed research on water resource issues. Institutes also use their base grants to help train new scientists, disseminate research results to water managers and the public, and to cooperate with other colleges and universities in their respective states and with other institutes and other organizations in their regions to promote regional coordination.*

*This project was also supported, in part, by General Purpose Revenue funds of the State of Wisconsin to the University of Wisconsin System for the performance of research on groundwater quality and quantity. Selection of projects was conducted on a competitive basis through a joint solicitation from the University and the Wisconsin Departments of Natural Resources; Agriculture, Trade and Consumer Protection; Commerce; and advice of the Wisconsin Groundwater Research Advisory Council and with the concurrence of the Wisconsin Groundwater Coordinating Council.*

# Effect of geochemical conditions on radium mobility in discrete intervals within the Midwestern Cambrian-Ordovician aquifer system

**A Final Report prepared for the State of Wisconsin Groundwater Research and Monitoring Program**

Madeleine Mathews[1], Madeline Gotkowitz[2,3], and Matthew Ginder-Vogel[1]

1. Environmental Chemistry and Technology, Department of Civil and Environmental Engineering, University of Wisconsin – Madison, Madison, WI
2. Wisconsin Geological and Natural History Survey, Madison, WI
3. Current Affiliation: Montana Bureau of Mines and Geology, Butte, MT

**Adapted from:** Mathews, Gotkowitz, and Ginder-Vogel (2018)

## Introduction

This report summarizes data and information gathering activities that examined Ra levels and aquifer geochemistry in the Madison, WI area for the period September 2016 through August 2017. The report is adapted from the published works of Mathews et al. (2018).

Radium (Ra) is a naturally occurring, radioactive contaminant present in many groundwater systems. Ingestion of Ra is a human health concern as it can accumulate in bone tissue where it continues to undergo radioactive decay. Long-term exposure may damage cell tissue, and is related to various types of bone disease (Canu et al., 2011; Evans, 1933; Guse et al., 2002; International Atomic Energy Agency, 2014; Mays et al., 1985; Moss et al., 1995; Rowland et al., 1978). The United States Environmental Protection Agency (EPA) regulates Ra in drinking water at a maximum contaminant level (MCL) for Ra in drinking water at 5 pCi/L for the combined total of isotopes, $^{226}$Ra and $^{228}$Ra (U.S. EPA, 2000).

Radium is produced in groundwater from the radioactive decay of parent elements uranium (U) and thorium (Th) (Figure S1-1) (Copenhaver et al., 1993; Gilkeson, 1984; International Atomic Energy Agency, 2014; B.C. Reynolds et al., 2003; Szabo et al., 2012; Tricca et al., 2001, 2000). These parent isotopes are common to fine-grained sedimentary deposits, such as shale and siltstone, and/or transition metal (e.g., Fe and Mn) (hydr)oxide coatings on mineral grains (Gilkeson et al., 1978; Grundl and Cape, 2006; International Atomic Energy Agency, 2014). Elevated concentrations of U and Th have also been observed in Precambrian crystalline bedrock (Mursky et al., 1989). Saline brines are also a possible source of dissolved U and Ra(II) to groundwater systems. During Pleistocene glaciation, increased pore pressure in the Lake Michigan basin resulting from the overlying Laurentide ice sheet may have driven saline groundwater west, providing a potential source of elevated Ra(II) concentrations in the eastern portion of the Midwestern C-O-AS (Siegel, 1990; Weaver and Bahr, 1991a; Winter et al., 1996).

Once in groundwater, Ra(II) mobility is largely controlled by sorption to transition metal (e.g., Fe and Mn) (hydr)oxide minerals and/or co-precipitation with barite ($BaSO_4$). These processes are affected by local aquifer geochemical conditions (Gilkeson et al., 1978; Tricca et al., 2000; Vinson et al., 2012). For example, in the Midwestern C-O-AS, elevated dissolved Ra(II) is generally correlated with low pH, low dissolved oxygen (DO), and high total dissolved solids (TDS) (Ayotte et al., 2011; Gilkeson, 1984; Grundl and Cape, 2006; Krishnaswami et al., 1991; Stackelberg et al., 2018; Szabo et al., 2012; Tomita et al., 2010; U.S. Department of the Interior and U.S. Geological Survey, 2012; Vinson et al., 2013, 2009). Reducing conditions are often associated with elevated dissolved Ra(II), because these conditions are less favorable for forming transition metal (hydr)oxides (Ayotte et al., 2011; Burghardt and Kassahun, 2005; Gonneea et al., 2008; Nathwani and Phillips, 1979; B.C. Reynolds et al., 2003; Stackelberg et al., 2018; Szabo et al., 2012; Tricca et al., 2001). Elevated ionic strength is also associated with elevated dissolved Ra(II) due to sorption-site competition (Szabo et al., 2012; Wilson, 2012). Within sulfate-rich, oxic aquifer systems, such as a regionally unconfined portion of the Midwestern C-O-AS in southeast Wisconsin, co-precipitation with $BaSO_4$ limits dissolved Ra(II) (Grundl and Cape, 2006; Szabo et al., 2012).

Elevated dissolved Ra(II) is common to the Midwestern C-O-AS, associated with anoxic conditions and elevated ionic strength (Stackelberg et al., 2018; Szabo et al., 2012). Similar trends are observed throughout Wisconsin (Grundl and Cape, 2006; Stackelberg et al., 2018; Vinson et al., 2018). However, these studies rely on water samples collected from municipal wells with long screened intervals (hundreds of meters), resulting in water produced from multiple hydrostratigraphic units (Grundl and Cape, 2006; Stackelberg et al., 2018; Szabo et al., 2012;

Vinson et al., 2012, 2009; Weaver and Bahr, 1991a). The geologic source of Ra could not be related to specific strata within the groundwater system.

This study investigates sources of dissolved Ra(II) within discrete hydrostratigraphic units in the Midwestern C-O-AS near Madison, Wisconsin, where the upper and lower sandstone aquifers are separated by a locally-confining shale aquitard (Weaver and Bahr, 1991a; Young and Siegel, 1992). Possible sources of Ra to groundwater include Ra-bearing aquifer solids, such as oxide rinds on silicate minerals; shales or other fine-grained, interbedded strata enriched in parent isotopes; and deep brines (Gilkeson et al., 1983; Grundl and Cape, 2006; Siegel, 1990; Sturchio et al., 2001; Vinson et al., 2009; Weaver and Bahr, 1991b). Here, we use a network of twenty-one short-screened monitoring wells, at depths ranging from 12 to 139 m, to sample for for $^{226}$Ra, $^{228}$Ra, $^{238}$U, $^{232}$Th, ionic composition, pH, specific conductance, and DO (Figure 1). The elemental composition of aquifer solids is also determined. These data provide insight into the geologic sources of Ra and the geochemical conditions that promote the mobility of Ra(II) within discrete hydrostratigraphic intervals.

## Project Objectives

The goal of this project was to develop a geochemical model describing the relationship of Ra to specific aquifer solids, in order to provide increased scientific understanding for strategies to minimize Ra in groundwater used as a drinking water source. The specific objectives and the work to achieve them is discussed below:

1. Investigate the isotopic signature of $^{226}$Ra and $^{228}$Ra in groundwater from the Midwestern Cambrian-Ordovician aquifer system to determine potential sources.
2. Quantify potential solid-phase sources of Ra, and parent nuclides U and Th. This includes studying nuclide speciation, dissolution, and/or sorption potential in these same solids
3. Provide a geochemical basis for management decisions regarding amelioration of high Ra levels in municipal wells

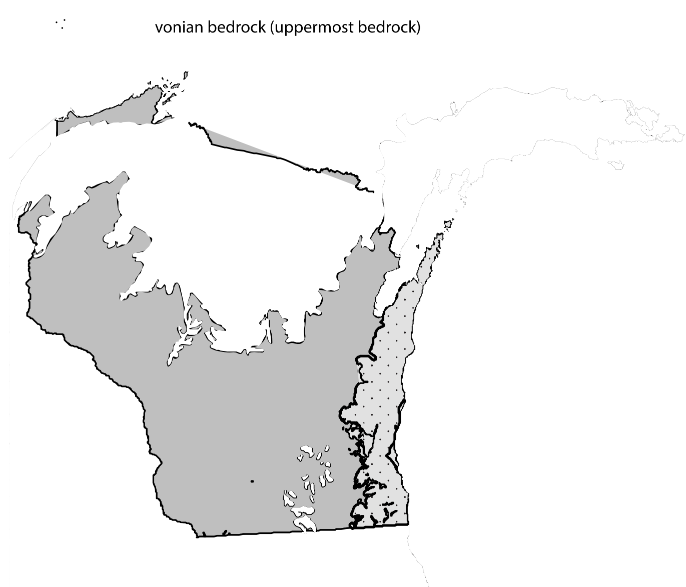


Figure 1. Extent of the Cambrian-Ordovician aquifer in Wisconsin. The Maquoketa shale underlies the Silurian-Devonian bedrock to the east, but forms the uppermost bedrock over a narrow area west of the Silurian. The inset map shows distribution of study sites; each site hosts multiple wells at various depths.

## Materials and Methods

*Regional hydrogeology*

As discussed in Young and Siegel, 1992, the Midwestern C-O-AS extends across much of the Midwestern United States, including parts of Minnesota, Wisconsin, Iowa, Missouri, and Illinois. It consists of a complexly layered sequence of sedimentary aquifers with interbedded confining units, overlain by unconsolidated glacial drift. Crystalline Precambrian rock forms the base of the system, and is overlain by marine-deposited Paleozoic sandstones, dolostones, and shales. These formations range from the Late Cambrian to Late Devonian age, with stratigraphic units increasing in thickness away from the arches and toward basins. In Wisconsin, these layered sedimentary sequences slope from the Wisconsin Arch toward the Michigan basin in the east, the Illinois basin in the south, and toward Iowa and Minnesota to the west. The Maquoketa Shale confines much of the Midwestern C-O-AS in eastern Wisconsin, but it is absent in central and western Wisconsin (Figure 1) (Young and Siegel, 1992).

*Local hydrogeology and sampling sites*

This study examines Ra(II) concentration and groundwater geochemistry in the Midwestern C-O-AS near Madison, Wisconsin characterize the C-O-AS as about 250 m thick in this region (Parsen et al., 2016). Relatively impermeable Precambrian crystalline rock forms the base of the Cambrian groundwater system and is overlain by the coarse- to medium-grained sandstone of the Mount Simon Formation. The Eau Claire Formation, which overlies the Mount Simon, consists of an upper sandstone facies underlain by interbedded siltstone and shale layers. These fine-grained deposits make up the locally extensive Eau Claire aquitard, which varies from 0 to 15 m in thickness across the greater Madison region. The aquitard restricts the exchange of water between the overlying formations the underlying Mount Simon sandstone (Figure 2). The dolomitic Eau Claire sandstone forms the base of the upper bedrock aquifer, and is overlain by quartz sandstone of the Wonewoc Formation and glauconitic sandstone of the Tunnel City Formation. In upland areas, the water table lies within the upper-most bedrock formations. In low-lying areas near the lakes and streams, the water table is relatively shallow and lies within saturated fine-grained till and lacustrine sediment that overlie bedrock. Land use in the study area is principally urban, and is surrounded by agricultural areas. Extensive pumping for regional water supplies has reversed pre-development conditions, resulting in downward hydraulic gradients from the upper, unconfined aquifer to the deep, confined aquifer over much of the study area (Parsen et al., 2016).

A network of twenty-one monitoring wells, with screen lengths ranging from 1.5 to 6.0 m, were sampled during this study. The wells are distributed across eight field sites in the greater Madison area, with six of these sites associated with near-by municipal wells (Figure 1). Each of the field sites hosts two monitoring wells at various depths, with the exception of MW-7, which has three monitoring wells, and the Sentry Well (SI Table 1, Figure 2). The Sentry Well contains a FLUTe$^{TM}$ multi-level sampling device that consists of six sampling ports at a variety of depths isolated from each other with hydraulic seals. The well network was installed for an unrelated study; construction details are described in (Gotkowitz et al., 2016). The monitoring wells target specific hydrostratigraphic units, and are completed in the Tunnel City Formation (n = 10), the Wonewoc Formation (n = 6), the Eau Claire aquitard (n = 1), and the Mount Simon Formation (n = 4). Wells completed above the aquitard are referred to as unconfined. Wells screened within or below the aquitard are described as "confined". Dedicated gas displacement pumps were used to purge and collect samples from the ports of the Sentry Well. A submersible electric pump was used to sample all other wells.

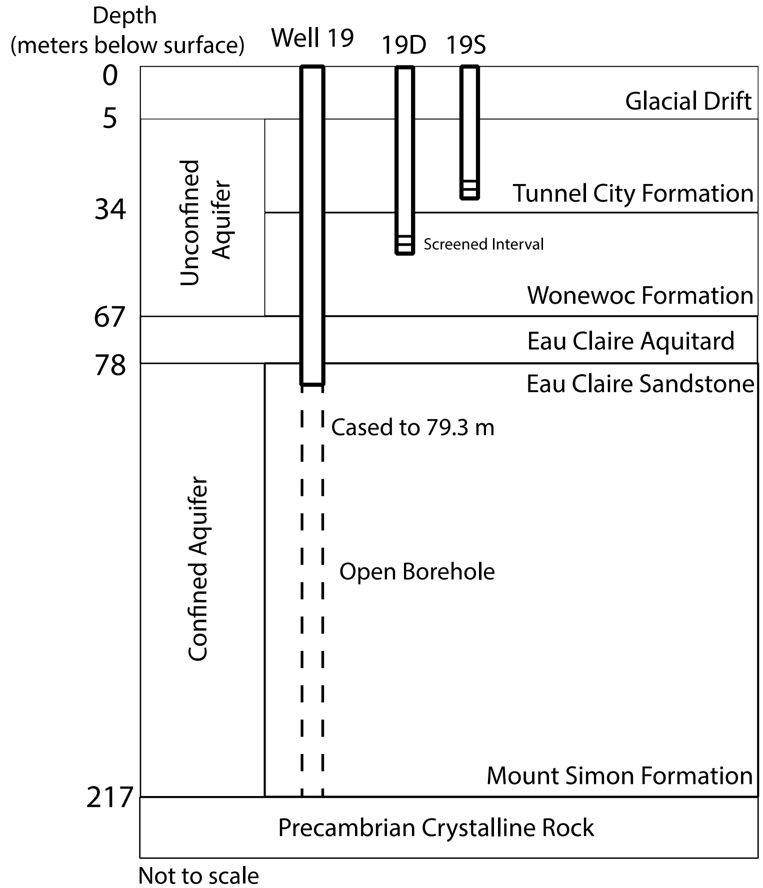


Figure 2. Representative hydrostratigraphy and well construction at the municipal well field site. Municipal wells such as Well 19 are open boreholes below the casing, while monitoring wells like MW-19D and MW-19S are screened across short intervals within hydrostratigraphic

*Groundwater characterization*

During the fall of 2016, all twenty-one monitoring wells in the study were sampled. A subset of thirteen wells were sampled a second time, in spring 2017. These wells were selected to include wells above and below the aquitard. Prior to sample collection, monitoring wells were purged of approximately 10 well volumes using a stainless-steel submersible pump. Sentry well (SW) ports were purged a minimum of five times over a two-day period prior to sample collection.

During both sampling campaigns, pH, temperature, and specific conductance were measured in the field following purging. DO was also measured in a flow-through cell during the second round of sampling. Samples for Ra(II) analysis were not filtered, to remain consistent with compliance sampling methods required of municipal water supply systems and preserved with concentrated nitric acid to pH $\leq 2$. Samples for aqueous analysis were field-filtered (0.45 μm), and acid preserved (pH $\leq 2$) at 4 °C until further analysis for dissolved metals and inorganic ions. Prior to dissolved metal analysis, samples were acidified with concentrated nitric acid to pH $\leq 2$. Analysis for uranium ($^{238}U$) and thorium ($^{232}Th$) was conducted on samples collected during the second round of sampling.

$^{226}Ra$ and $^{228}Ra$ analyses were conducted by Eurofins Eaton Analytical, Inc. in a manner consistent with the Georgia Tech method (Georgia Institute of Technology, 2004). Radium values at or below the instrumental detection level have been designated as Minimum Detectable Activity (MDA) or < MDA, and are represented as 0 pCi/L on figures; the MDA is the concentration which can be measured with ± 100 % certainty at the 95 % confidence level. Analysis of $^{238}U$ and $^{232}Th$ was conducted using a ThermoScientific ELEMENT2 High Resolution inductively coupled plasma mass spectrometer (Table S1-1). A Dionex ICS-2100 ion chromatography system was used to determine the concentration of nitrate ($NO_3^-$), sulfate ($SO_4^{2-}$), and chloride ($Cl^-$) in water samples (Table S1-1). A PerkinElmer Optima 4300 DV inductively-coupled plasma optical emission spectrometer was used to quantify dissolved barium ($Ba^{2+}$), calcium ($Ca^{2+}$), iron ($Fe^{2+}$), magnesium ($Mg^{2+}$), manganese ($Mn^{2+}$), and sodium ($Na^+$) in aqueous samples (Table S1-1). Tritium ($^3H$) concentrations were compiled from previous studies conducted at these wells by the Wisconsin Geological and Natural History Survey (WGNHS) (Table S1-2) (Gotkowitz, 2015).

A quality control sample was collected during each sampling round to evaluate the potential contribution of Ra(II) from field equipment. Control samples were collected by flushing the submersible pump and tubing with 40 liters of ultrapure water followed by collection of 4 L of ultrapure water for analysis. Sample MW-PL1 was collected through the entire length of the tubing in 2016, while MW-PL2 was collected through a short length (5 m) of tubing.

*Solid-phase characterization*

Aquifer solids were selected from well cuttings archived at the WGNHS. Cuttings, collected during the construction of municipal well 19 in 1969, were available at 1.5 meter intervals from surficial glacial drift to the Precambrian crystalline bedrock at 219 m below ground surface (Figure 2). Cuttings were prepared by placing in a medical grade polyethylene sample container, with a piece of 4.0 μm polypropylene thin film secured across the vial top by a rubber band. Elemental composition was determined using a Thermo Fisher Niton XL3t GOLDD+ hand-held X-ray fluorescence (XRF) analyzer. The vial was turned to allow cuttings to rest on the film across the XRF stage (Rowe et al., 2012; Zambito et al., 2016).

XRF analysis was conducted in "Test All Geo" mode, using the 8 mm aperture opening and a 50 kV beam, following established procedures (Zambito et al., 2016). A 105 second total filter duration-time (main filter 30 s, light filter 30 s, low filter 30 s, and high filter 15 s) was applied to each sample. XRF analysis was monitored using standards from the United States Geological Survey (USGS) for shale, carbonate, and quartz sandstone. Minimum detection limits for Ra parent isotopes were 1.24 ppm for thorium and 2 ppm for uranium (Haas et al., 2017). Geologic and geophysical logs available from the WGNHS were compared with the XRF results to identify the depth and thickness of hydrostratigraphic intervals.

## Results

Groundwater chemical composition over the two sampling periods is summarized in SI Table 1. The pH of the samples ranged from 6.3 to 7.7, while the specific conductance values ranged from 510 to 3030 μS/cm. Tritium, an indicator of groundwater age, ranged from < 0.8 to 11 ± 2 TU in the unconfined aquifer and from < 0.8 to 5.3 ± 0.6 TU in the confined system (Figure 3, Table S1-2).

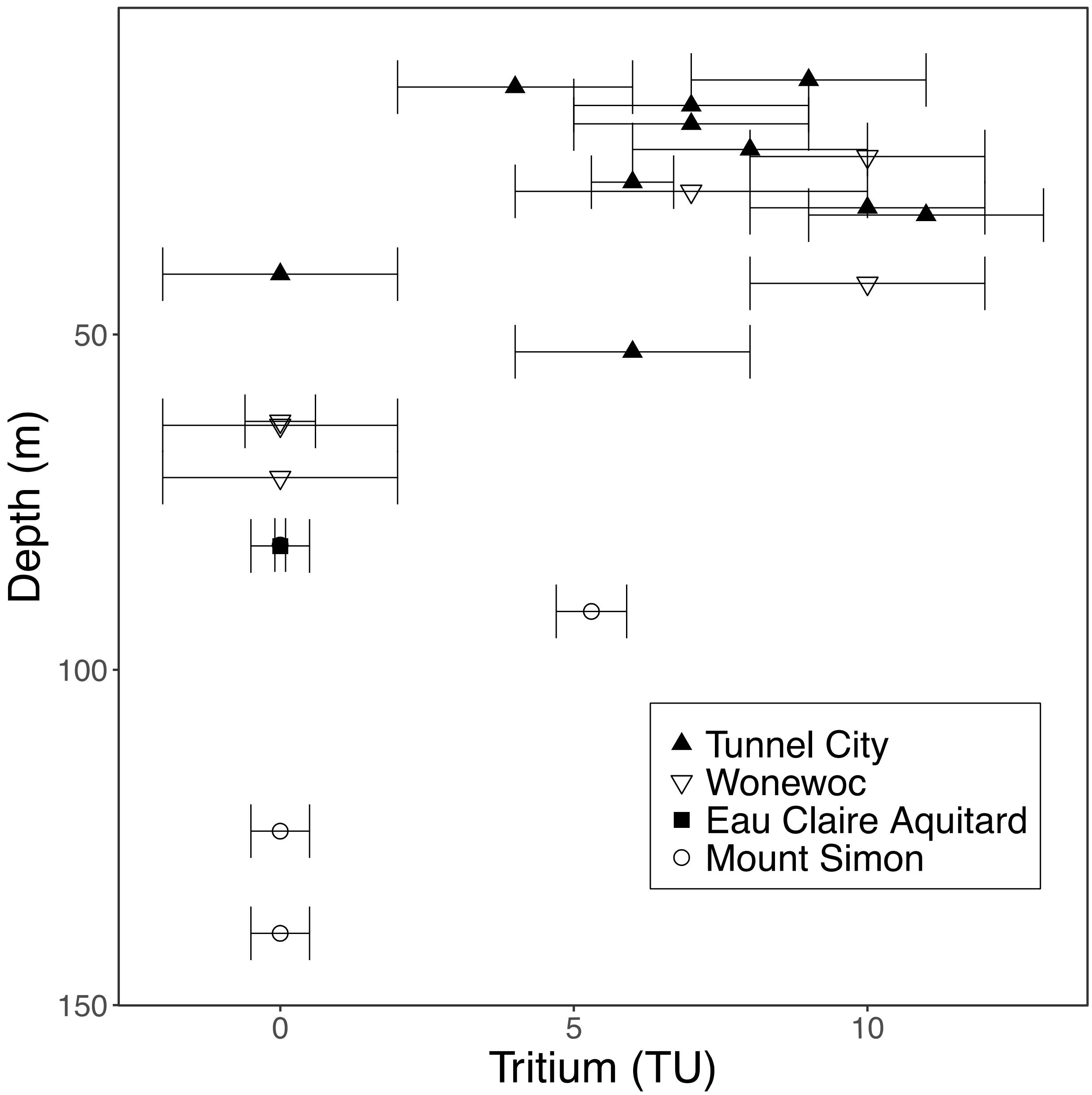

Figure 3. Tritium concentration at depth from surface, differentiated by hydrostratigraphic unit (Gotkowitz, 2015).

The DO concentration in groundwater varied between the upper aquifer and the underlying confined aquifer (SI Table 2). Based upon these measurements, 18 wells were oxic (DO ≥ 0.5 mg/L, Mn(II) < 0.05 mg/L), 1 well suboxic (DO < 0.5 mg/L, Mn(II) < 0.05 mg/L), and 2 wells anoxic (DO < 0.5 mg/L, Mn(II) ≥ 0.05 mg/L). In the confined aquifer, DO ranged from 0.04 to 5.46 mg/L, and Ra(II) ranged from < MDA 95 to 4.6 pCi/L. In the unconfined aquifer, DO concentrations ranged from 2.13 to 10.64 mg/L, and Ra(II) ranged from < MDA 95 to 5.2 pCi/L. Ra generally increased with increasing DO (Figure 4).

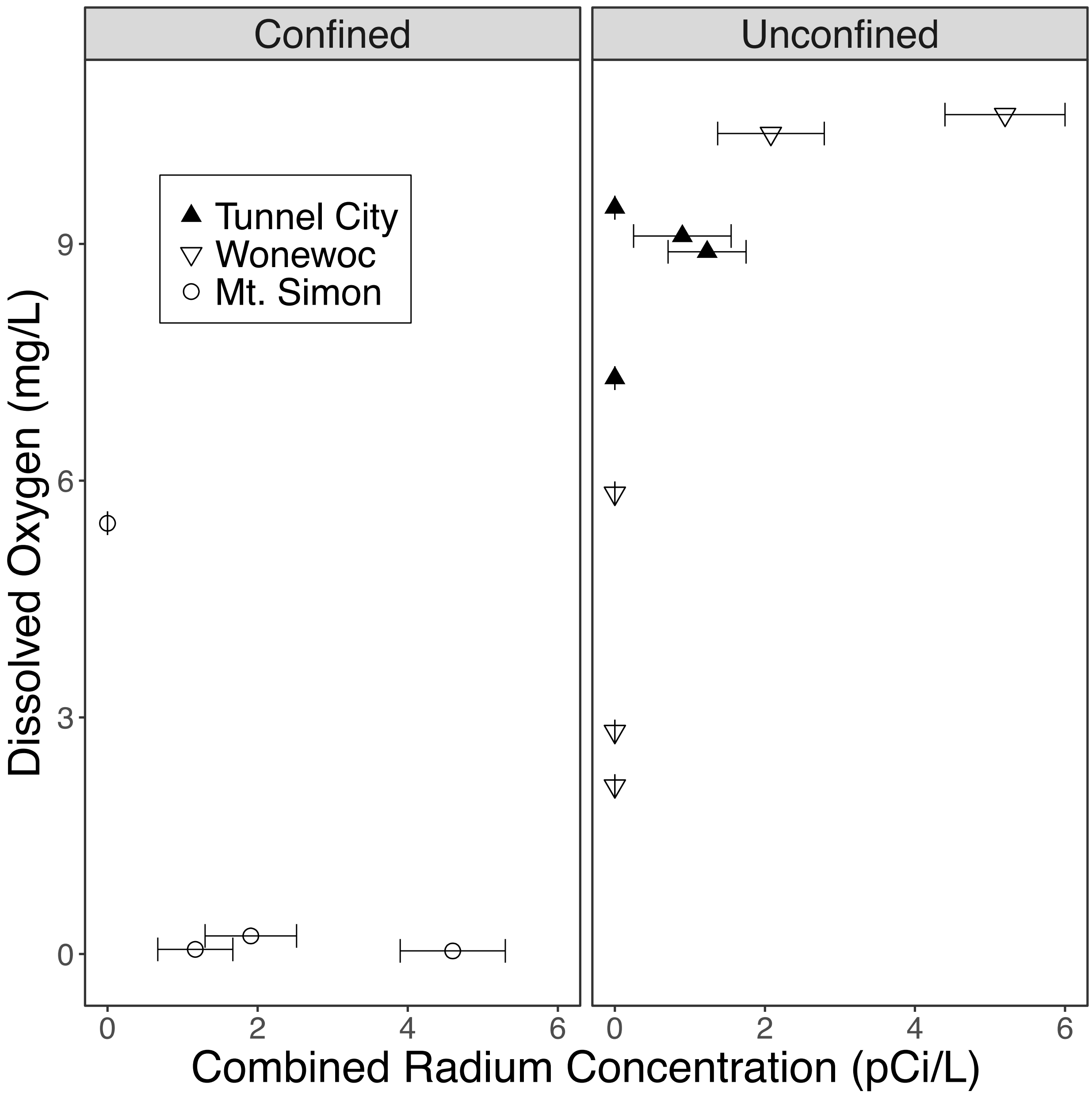


Figure 4. The relationship between combined radium concentration ($^{226}Ra + ^{228}Ra$) and DO from spring 2017 sampling, distinguished by hydrostratigraphic unit and aquifer designation. Error estimates are shown for combined Ra(II) concentrations above minimum detectable activity at the 95 % confidence level (MDA 95); values at or below MDA 95 are represented as 0 pCi/L.

Overall, concentrations of parent isotopes $^{238}U$ and $^{232}Th$ were low in groundwater. Aqueous $^{238}U$ concentrations ranged from 0.0004 ± 0.0000 to 5.3 ± 0.1 µg/L, while $^{232}Th$ ranged from non-detectable to 0.005 ± 0.002 µg/L (Figure 5). The highest $^{238}U$ concentration, 5.27 ± 0.1 µg/L, was collected from the Mount Simon, just below the Eau Claire aquitard, in well LE-VD.

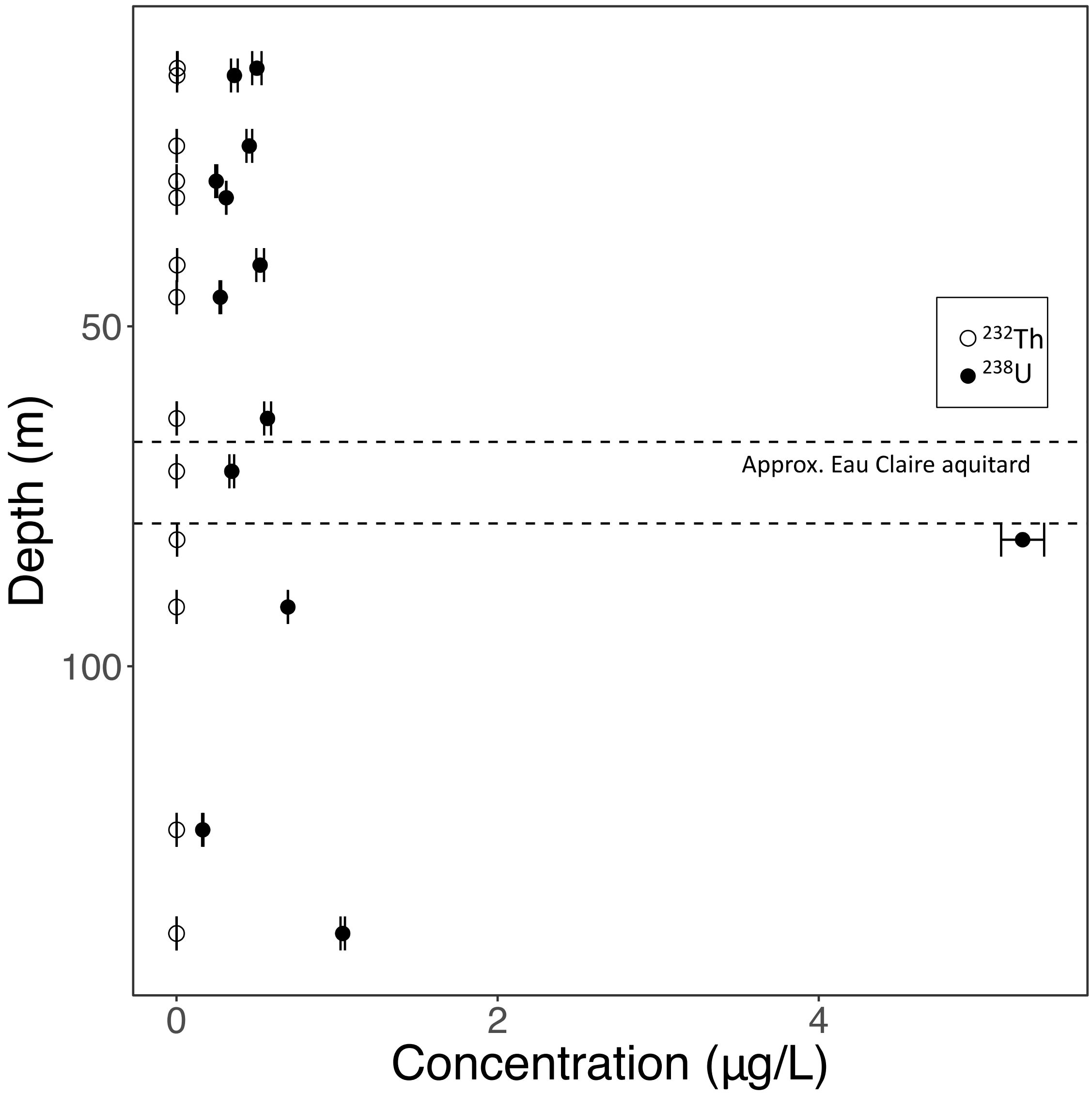


Figure 5. Aqueous concentrations of Ra parent isotopes, $^{238}U$ and $^{232}Th$, as a function of depth below ground surface.

In this study, combined Ra(II) concentrations less than 1.10 ± 0.54 pCi/L were considered below the limit of quantification, due to the presence of combined Ra(II) concentration in control sample MW-PL1. The combined Ra(II) concentration in most groundwater samples ranged from non-detectable to 2.2 pCi/L, with two wells, MW-19D and SW – port 6, exceeding this range (Figure 6). Wells with Ra(II) exceeding detection levels in spring 2017 were at concentrations within the error bounds reported from the fall 2016 samples, and other samples exhibited little variation. Both samples collected from well MW-19D, screened in the Wonewoc sandstone, contained 5.2 pCi/L Ra(II); all other samples completed in the unconfined aquifer had Ra(II) concentrations less than the MCL. Dissolved Ra(II) in well SW – port 3, the only well associated with the Eau Claire aquitard, was below the MDA. Among samples from the Mount Simon sandstone, the highest combined Ra(II) concentration, 4.6 ± 0.7 pCi/L, was collected from the deepest well, SW–port 6, at 139 m at depth.

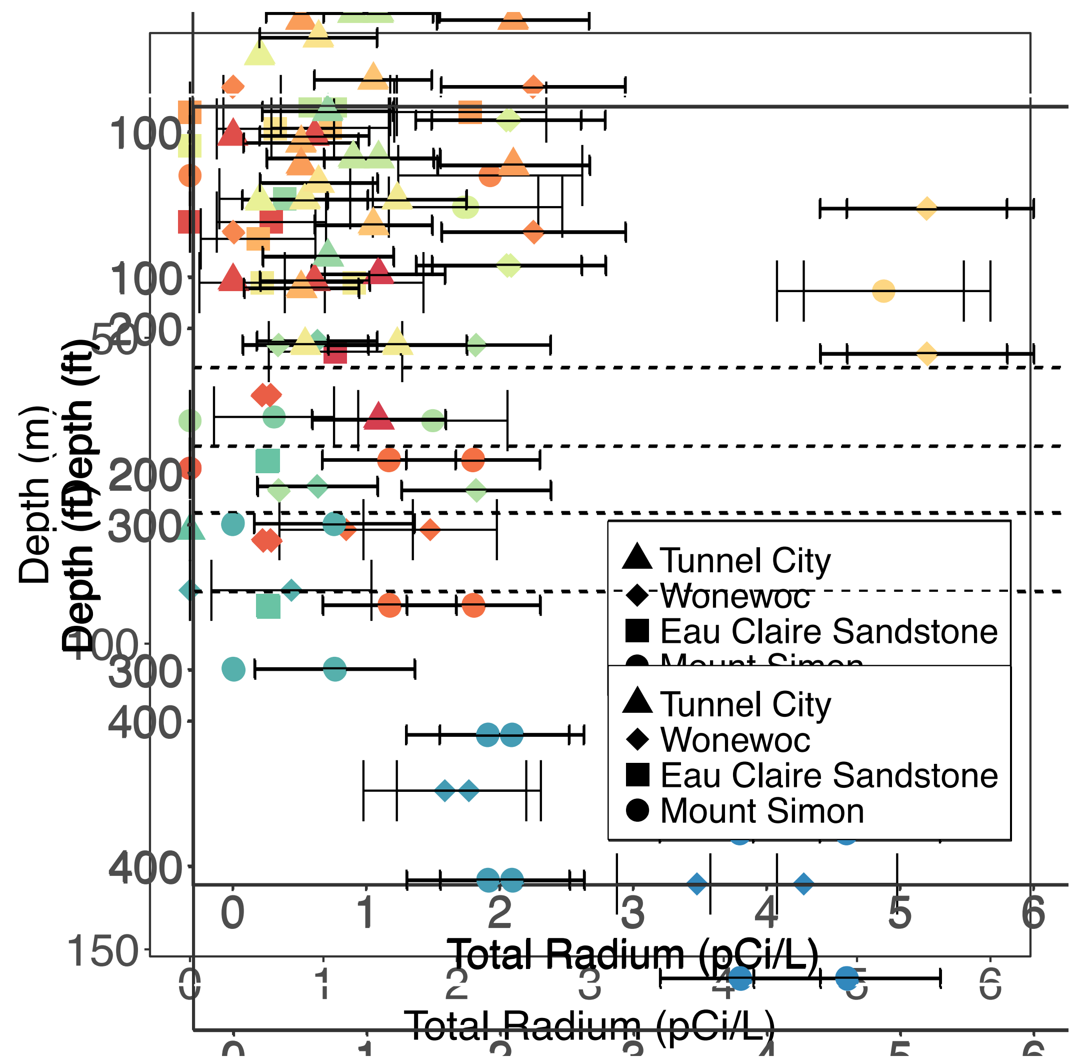


Figure 6. Combined radium concentration ($^{226}Ra+^{228}Ra$) by well depth from both sampling periods. Results from wells sampled twice to examine replicability are shown with the same color. Dissolved Ra(II) values at or below minimum detectable activity at the 95 % confidence interval (MDA 95) are plotted at 0 pCi/L.

Specific conductance, used here as an indicator of total dissolved solids, varied widely in groundwater, from 510 to 3030 μS/cm. The highest concentrations of $Ca^{2+}$ (max. 223 mg/L at 12 m-depth), $Cl^{-}$ (max. 662 mg/L at 12 m-depth), $Mg^{2+}$ (max. 116 mg/L at 29 m-depth), $Na^{+}$ (max. 237 mg/L at 29 m-depth), and $SO_4^{2-}$ (max. 79 mg/L at 12 m-depth) were observed in wells completed in the unconfined aquifer. Major ion concentrations decreased with depth (Figure 7) as did specific conductance, which ranged from 570 to 860 μS/cm in wells completed in the confined system.

In general, there is a weak correlation between Ra(II) concentration and specific conductance in the Wonewoc sandstone ($r^2 = 0.54$) and the Tunnel City stratigraphic unit ($r^2 = 0.25$; Figure 8). Estimated $Ba^{2+}$ activities, calculated according to the method described in (Brezonik and Arnold, 2011), did not vary significantly (p-value = 0.34) as a function of aquifer formation (Table S1-1). The calculated barite saturation index (SI) does not exceed a value of 1 for any of the samples collected in this study (Calculations S4, Figure S1-2). While $Ba^{2+}$ concentration increased as sulfate concentration increased within the Wonewoc, this trend was not observed in groundwater from the Tunnel City unit (Figure S1-2).

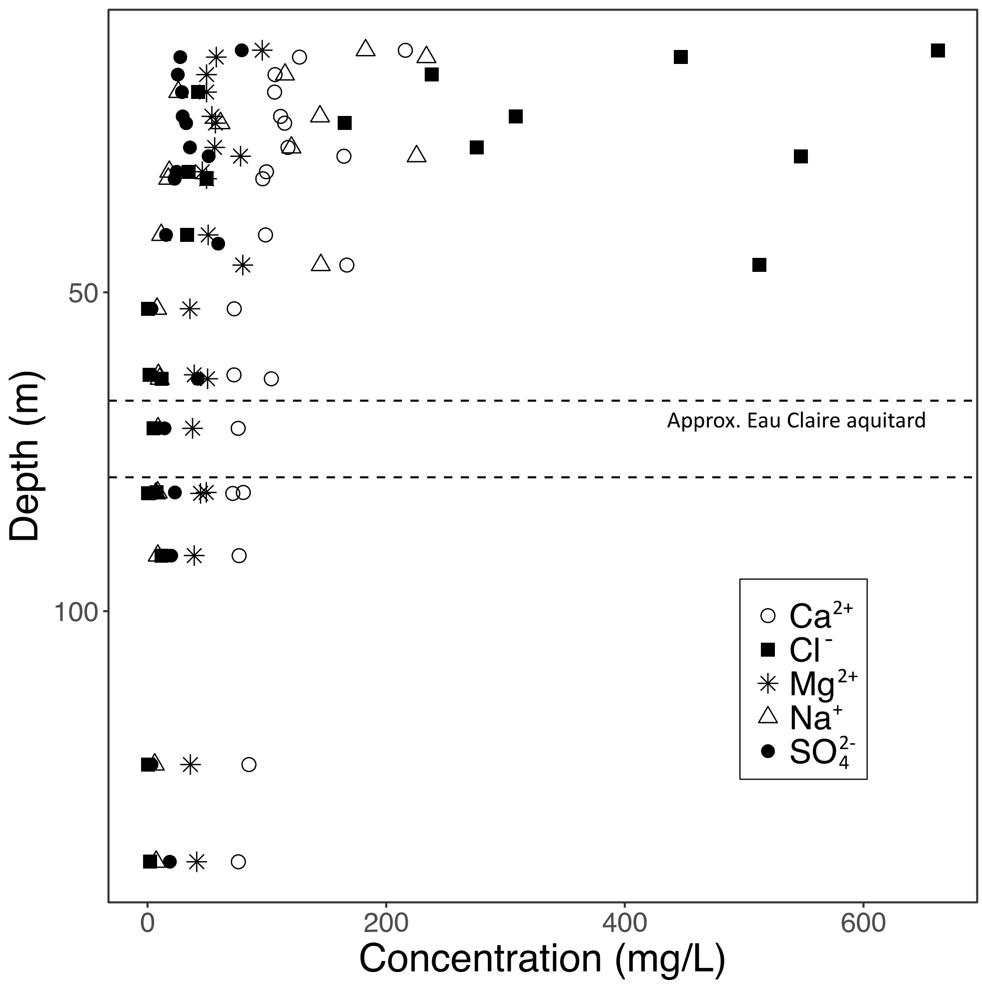


Figure 7. Concentration of major ions versus depth from surface, from monitoring wells in Madison, WI from 2016 samples.

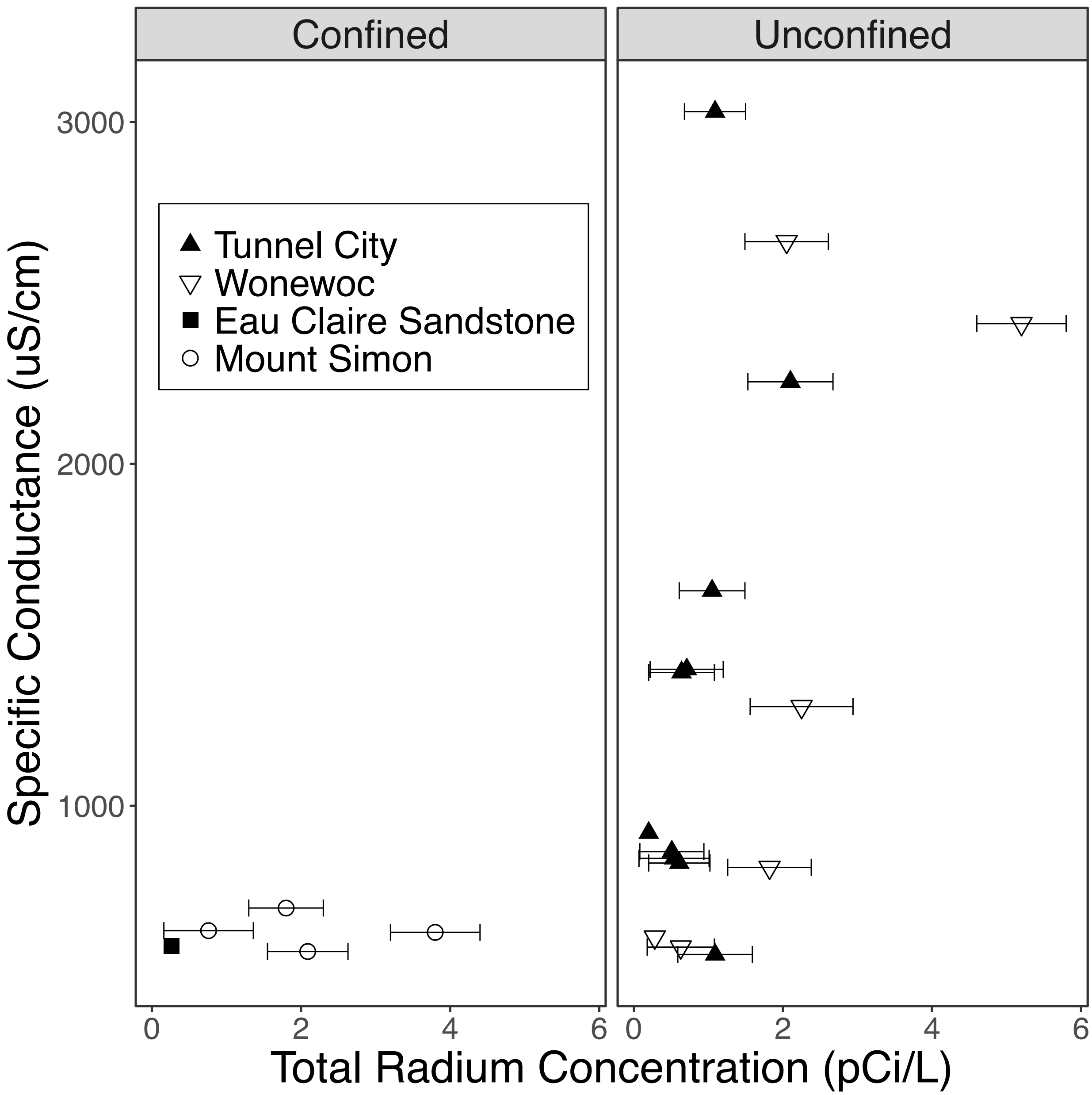


Figure 8. The relationship between combined radium ($^{226}Ra + ^{228}Ra$) and specific conductance from fall 2016 sampling, distinguished by hydrostratigraphic units and aquifer designation. Ra(II) concentrations at or below the minimum detectable activity at the 95 % confidence interval (MDA 95) are represented as 0 pCi/L.

XRF analyses of aquifer solids from municipal well 19 demonstrate the heterogeneity of elemental composition within discrete stratigraphic horizons (Figure 9). Primary elements at the study site include Si (median 29.6, ranging 7.9 to 44.8 % by weight), Ca (median 3.6, ranging 0.02 to 19.81 % by weight) and Mg (median 0.70, ranging 0 to 17 % by weight), where 1 % by weight = 10,000 parts per million (ppm). Samples with elevated K and Al indicate clay mineralogy (e.g., 67 to 78 m below the surface) and correspond to the depth of the Eau Claire aquitard at well 19. Elevated Fe concentrations appear in the Wonewoc Formation (median 0.24, ranging 0.02 to 3.67 % by weight), the Eau Claire Formation (median 1.14, ranging 0.18 to 2.67 % by weight), and the Mount Simon Formation (median 0.11, ranging 0.02 to 6.33 % by weight). Manganese concentrations in aquifer solids are more consistent, with a median of 0.02 % by weight over the groundwater system, ranging 0 to 0.15 % by weight. Solid-phase concentrations of U (median 8.47, ranging 0 to 9.68 ppm) and Th (median 4.96, ranging 0 to 8.36 ppm) are notable in the Eau Claire aquitard (Figure 9). Elevated concentrations of U and Th were also observed at several depths in both the Wonewoc (U median 0, ranging 0 to 14 ppm; Th median 0, ranging 0 to 14.63 ppm) and Mount Simon sandstones (U median 0, ranging 0 to 29.95 ppm; Th median 0, ranging 0 to 27.94 ppm; Figure 9).

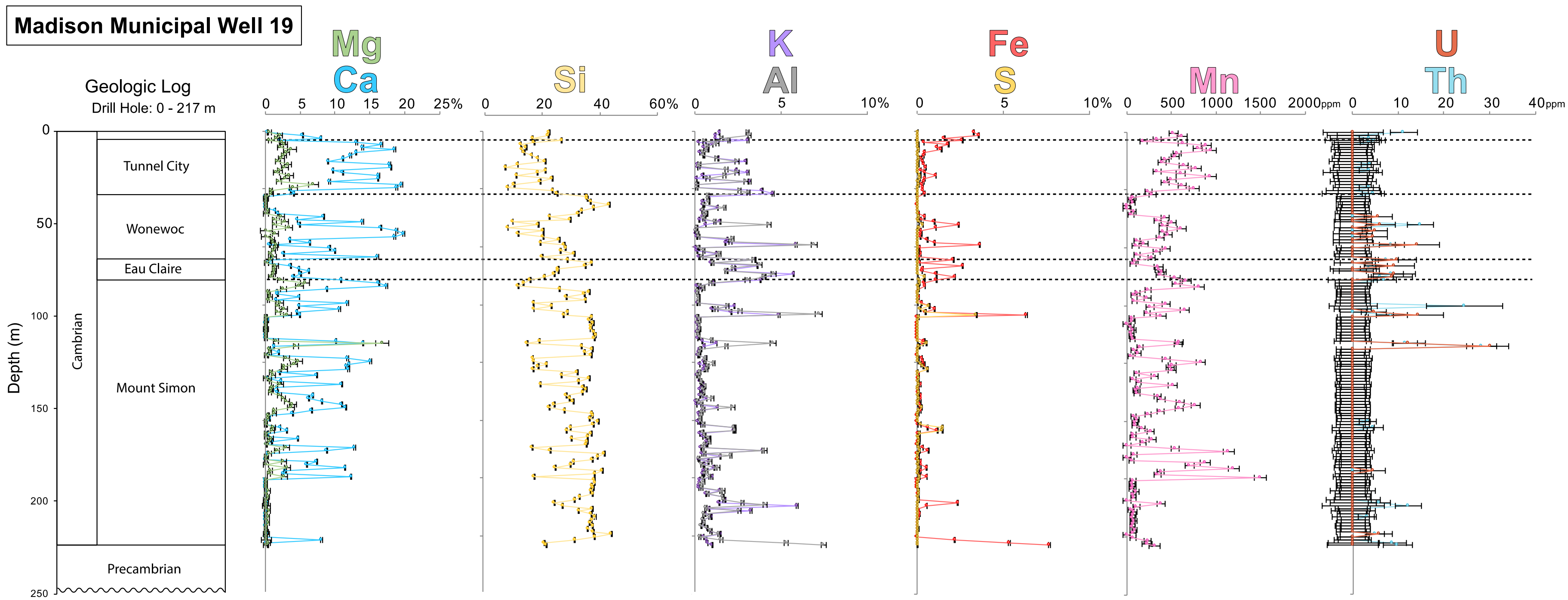


Figure 9. Solid-phase elemental composition from X-ray fluorescence analysis of municipal well 19. Concentration scales differ for each element grouping. Elemental weight abundance is either presented as parts per million (ppm) or weight percent (%), defining 1 % = 10,000 ppm.

## Discussion

This study focuses on determining dissolved Ra(II) concentrations in discrete hydrostratigraphic intervals within a locally-confined region of the Midwestern C-O-AS, in order to build upon studies that rely on data from wells with long open intervals (Grundl and Cape, 2006; Stackelberg et al., 2018; Szabo et al., 2012; Vinson et al., 2012, 2009; Weaver and Bahr, 1991a). In this study, a majority of monitored depths had Ra(II) concentrations below background levels, but differences in geochemical conditions appear to result in locally elevated Ra.

Low DO, low pH, and/or high specific conductance in groundwater systems are often correlated with Ra(II) concentrations above the MCL, both in general and within the Midwestern C-O-AS (Ayotte et al., 2011; Gilkeson, 1984; Grundl and Cape, 2006; Krishnaswami et al., 1991; Stackelberg et al., 2018; Szabo et al., 2012; Tomita et al., 2010; U.S. Department of the Interior and U.S. Geological Survey, 2012; Vinson et al., 2013, 2009). Groundwater in the study area is relatively neutral in pH (e.g., 6.3 to 7.7), and Ra(II) mobilization due to acidic conditions is unlikely (SI Table 1). The two wells with elevated dissolved Ra(II) are dissimilar (Figure 6, SI Table 1). One is under oxic conditions with elevated specific conductance, while the second is completed in the confined aquifer, under anoxic and low dissolved solids conditions. This suggests that multiple factors contribute to elevated Ra(II) in this setting.

Radium parent radionuclides ($^{238}$U and $^{232}$Th) are found in association with fine-grained sedimentary layers, including shale aquitards, or oxide coatings on mineral grains (Gilkeson et al., 1983; Grundl and Cape, 2006; Senior and Vogel, 1995; Sturchio et al., 2001; Weaver and Bahr, 1991a). Aqueous and solid-phase parent radionuclide concentrations were relatively low throughout most of the stratigraphic section in the study area (Figures 5, 9). The solid-phase composition varied with depth; higher concentrations of U and Th occur in the Eau Claire aquitard, and the Wonewoc and Mount Simon Formations contained elevated U and Th peaks (Figure 9). Since U and Th are present in the unconfined and confined aquifers, and the Eau Claire aquitard, production of Ra(II) via radioactive decay from U and Th can occur in any of these hydrostratigraphic units. However, shale layers, although enriched in parent nuclides, tend to have relatively low dissolved Ra(II) due to their high sorption capacity (Gilkeson, 1984; Gilkeson et al., 1978; Szabo et al., 2012). This is consistent with the less than detectable level of combined dissolved Ra(II) from SW – port 3, completed within the Eau Claire aquitard (Figure 6).

The $^{3}$H content of water is a general indicator of groundwater age. Eight wells produced water with low tritium (< 0.8 TU), suggesting that these wells produce old (pre-1950) (Table S1-2). Thirteen wells produced water with tritium > 4 TU, indicating more recent recharge, since 1950 (Stackelberg et al., 2018). The two wells with dissolved Ra(II) above 3 pCi/L differ with respect to tritium. Tritium at MW-19D, 10 ± 2 TU, indicates recently recharged groundwater, whereas tritium levels were less than detectable level in SW – port 6.

Radium partitioning to Fe and/or Mn (hydr)oxides can decrease aqueous Ra(II) concentrations (B. C. Reynolds et al., 2003; Szabo et al., 2012; Tricca et al., 2000). However, anoxic conditions contribute to Ra(II) mobility and an increase in concentrations, due to the absence or dissolution of these minerals (International Atomic Energy Agency, 2014; Szabo et al., 2012). In groundwater samples from the confined system, elevated Ra(II) was associated with low DO (Figure 4). In several samples obtained from the unconfined system, the DO content ranges from 2.1 to 7.3 mg/L while Ra(II) remains undetectable. However, in five samples from the unconfined system with DO ≥ 8.9 mg/L, dissolved Ra(II) ranges from non-detectable to 5.2 pCi/L (Figure 4). Due to the oxic nature of the unconfined aquifer, the elevated levels of dissolved Ra(II) in the unconfined aquifer are not likely due to the absence of Fe and Mn (hydr)oxides (Szabo et al., 2012). Additionally, there was no evidence of elevated $^{238}U$ or $^{232}Th$ in the unconfined aquifer (Table S1-1). This suggests that elevated dissolved Ra(II) in the unconfined aquifer is likely due to other geochemical conditions, discussed below.

Other studies indicate that elevated dissolved Ra(II) correlates with elevated ionic strength (Nathwani and Phillips, 1979; Oden and Szabo, 2016; Sajih et al., 2014; Tomita et al., 2010). In this study, concentrations of $Ca^{2+}$, $Cl^{-}$, $Mg^{2+}$, $Na^{+}$, and $SO_4^{2-}$ were elevated in groundwater in the Tunnel City and Wonewoc hydrostratigraphic units (Figure 7). Increased specific conductance was also observed with elevated combined Ra(II) concentration in the unconfined aquifer (Figure 8). Despite the large range in TDS, water in all wells remained undersaturated with respect to $BaSO_4$ (Figure S1-2). This indicates that $BaSO_4$ formation is likely not an important factor in controlling Ra(II) concentration in this setting (Grundl and Cape, 2006; Stackelberg et al., 2018; Szabo et al., 2012).

Geochemistry in the monitoring well pair, MW-19S and MW-19D, differ from each other. These wells, installed within 10 m of each other, are completed in the unconfined aquifer at depths of 16 and 42 m, respectively. The deeper well, MW-19D, contained 5.2 pCi/L combined Ra(II), the highest concentration amongst the study wells, while Ra(II) was below the detection limit at MW-19S (SI Table 1). Consistent with greater Ra(II) mobility associated with elevated ionic strength, MW-19D had higher $Cl^{-}$, and TDS, than MW-19S. This, in addition to higher tritium at MW-19D, suggests good connectivity from the water table to MW-19D (Gellasch et al., 2013; Gotkowitz, 2015). Elevated TDS and relatively young groundwater age at the deeper of the paired wells suggest the presence of a preferential pathway, such as a fracture, connecting MW-19D to the water table (Gellasch et al., 2013; Parsen et al., 2016). Such fractures in the Tunnel City and Wonewoc Formations are well documented in the study area (Gellasch et al., 2013; Parsen et al., 2016). These results indicate that groundwater quality in the upper aquifer is affected by chloride-rich urban storm water impacted by sanitary sewers and/or road salt. Although the direct contribution of dissolved Ra(II) from infiltration of storm water cannot be ruled out, the elevated TDS correlated with greater dissolved Ra(II) in the unconfined aquifer supports increased Ra mobility due to sorption site competition. In contrast, absence of redox-sensitive minerals likely contributes to mobility of dissolved Ra(II) in the confined aquifer.

**Conclusions**

Results from the analyses of aquifer matrix and groundwater samples from discrete hydrostratigraphic units to further elucidate the controls on sources and movement of Ra in a locally confined area in the Midwestern C-O-AS. Overall, $^{238}U$ and $^{232}Th$ concentrations are relatively low in both aqueous and solid-phase samples analyzed as part of this study. However, despite the relatively low concentrations of parent isotopes, Ra(II) is mobile at discrete depths in both the upper, unconfined surface aquifer and the underlying confined aquifer. Anoxic conditions in the confined system likely result in the absence of Fe and Mn (hydr)oxides, resulting in limited Ra(II) sorption sites (Gilkeson et al., 1978; Tricca et al., 2000; Vinson et al., 2012). In wells in the unconfined aquifer that reflect the impact of surface processes (e.g., elevated specific conductance), elevated dissolved Ra(II) is attributed to sorption site competition. Although co-precipitation with $BaSO_4$ can limit dissolved Ra(II), geochemical measurements indicate that the formation of barite is not thermodynamically favorable in this system, and thus does not play an important role in controlling dissolved Ra(II) concentration.

This study utilized short-screened monitoring wells to characterize variability in the distribution of Ra(II) and identify potential Ra sources and sinks within specific hydrostratigraphic strata. Results demonstrate that background concentrations of dissolved Ra(II) in this region of the Midwestern C-O-AS range from non-detectable to 2.4 pCi/L. Multiple mechanisms, including absence (or dissolution) of Fe and Mn (hydr)oxide coatings and elevated dissolved ion content, apparently result in elevated Ra(II) within these discrete aquifer intervals. This study expands knowledge of the contribution of dissolved Ra(II) from distinct hydrostratigraphic units within the Midwestern C-O-AS. While low-levels of Ra are observed throughout the system, local changes in hydrostratigraphic geochemistry can result in elevated Ra(II) in the groundwater.

**Acknowledgements**

This study was funded by the University of Wisconsin Water Resources Institute. We thank the Madison Water Utility for their assistance and cooperation with this work. Uranium and thorium trace metal analyses were performed by the Wisconsin State Laboratory of Hygiene. Pete Chase, WGNHS, assisted with sample collection. We also thank Elizabeth Tomaszewki, Lily Schacht, and three anonymous reviewers for comments and recommendations that greatly improved this manuscript.

## References


Ayotte, J.D., Szabo, Z., Focazio, M.J., Eberts, S.M., 2011. Effects of human-induced alteration of groundwater flow on concentrations of naturally-occurring trace elements at water-supply wells. Appl. Geochemistry 26, 747–762. https://doi.org/10.1016/J.APGEOCHEM.2011.01.033

Brezonik, P.L., Arnold, W.A., 2011. Water chemistry : an introduction to the chemistry of natural and engineered aquatic systems.

Burghardt, D., Kassahun, A., 2005. Development of a reactive zone technology for simultaneous in situ immobilisation of radium and uranium. Environ. Geol. 49, 314–320. https://doi.org/10.1007/s00254-005-0093-0

Canu, I.G., Laurent, O., Pires, N., Laurier, D., Dublineau, I., 2011. Health effects of naturally radioactive water ingestion: the need for enhanced studies. Environ. Health Perspect. 119, 1676–80. https://doi.org/10.1289/ehp.1003224

Copenhaver, S.A., Krishnaswami, S., Turekian, K.K., Epler, N., Cochran, J.K., 1993. Retardation of 238U and 232Th decay chain radionuclides in Long Island and Connecticut aquifers. Geochim. Cosmochim. Acta 57, 597–603. https://doi.org/10.1016/0016-7037(93)90370-C

Evans, R.D., 1933. Radium poisoning: a review of present knowledge. Am. J. Public Heal. Nations Heal. 23, 1017–1023. https://doi.org/10.2105/AJPH.23.10.1017-b

Gellasch, C.A., Bradbury, K.R., Hart, D.J., Bahr, J.M., 2013. Characterization of fracture connectivity in a siliciclastic bedrock aquifer near a public supply well (Wisconsin, USA). Hydrogeol. J. 21, 383–399. https://doi.org/10.1007/s10040-012-0914-7

Georgia Institute of Technology, 2004. The determination of radium-226 and radium-228 in drinking water by gamma-ray spectrometry using HPGE or Ge(Li) detectors, revision 1.2.

Gilkeson, R.H., 1984. Isotopic studies of the natural sources of radium in groundwater in Illinois: University of Illinois, Water Resources Center Research Report, 187.

Gilkeson, R.H., Cartwright, K., Cowart, J.B., Holtzman, R.B., 1983. Hydrogeologic and Geochemical Studies of Selected Natural Radioisotopes and Barium in Groundwater in Illinois: University of Illinois, ISGS Contract/Grant Report 1983-6.

Gilkeson, R.H., Specht, S.A., Cartwright, K., Griffin, R.A., Larson, T.E., 1978. Geologic studies to identify the source for high levels of radium and barium in Illinois ground-water supplies: a preliminary report: University of Illinois, Water Resources Center Research Report 135.

Gonneea, M.E., Morris, P.J., Dulaiova, H., Charette, M.A., 2008. New perspectives on radium behavior within a subterranean estuary. Mar. Chem. 109, 250–267. https://doi.org/10.1016/J.MARCHEM.2007.12.002

Gotkowitz, M.B., 2015. Evaluating remedies for pathogen contamination of urban groundwater. PhD Dissertation, University of Wisconsin-Madison.

Gotkowitz, M.B., Bradbury, K.R., Borchardt, M.A., Zhu, J., Spencer, S.K., 2016. Effects of climate and sewer condition on virus transport to groundwater. Environ. Sci. Technol. 50, 8497–8504. https://doi.org/10.1021/acs.est.6b01422

Grundl, T., Cape, M., 2006. Geochemical factors controlling radium activity in a sandstone aquifer. Ground Water 44, 518–527. https://doi.org/10.1111/j.1745-6584.2006.00162.x

Guse, C.E., Marbella, A.M., George, V., Layde, P.M., 2002. Radium in Wisconsin drinking water: an analysis of osteosarcoma risk. Arch. Environ. Heal. An Int. J. 57, 294–303. https://doi.org/10.1080/00039890209601412

Haas, L., Zambito, J., Hart, D., 2017. Portable X-Ray Fluorescence (pXRF) Measurements of Uranium and Thorium in Madison, Wisconsin, Water Utility Wells 4 and 27: Wisconsin Geological and Natural History Survey, Open-File Report 2017-01.

International Atomic Energy Agency, 2014. The environmental behaviour of radium: revised edition. Tech. Reports Ser. No. 476 44–51. https://doi.org/10.1016/0883-2927(92)90073-C

Krishnaswami, S., Bhushan, R., Baskaran, M., 1991. Radium isotopes and 222Rn in shallow brines, Kharaghoda (India). Chem. Geol. Isot. Geosci. Sect. 87, 125–136. https://doi.org/10.1016/0168-9622(91)90046-Y

Mathews, M., Gotkowitz, M., & Ginder-Vogel, M. (2018). Effect of geochemical conditions on radium mobility in discrete intervals within the Midwestern Cambrian-Ordovician aquifer system. *Applied Geochemistry, 97*, 238-246. doi:https://doi.org/10.1016/j.apgeochem.2018.08.025

Mays, C.W., Rowland, R.E., Stehney, A.F., 1985. Cancer risk from the lifetime intake of Ra and U isotopes. Health Phys. 48, 635–47. https://doi.org/10.1097/00004032-198505000-00005

McMahon, P.B., Chapelle, F.H., 2008. Redox processes and water quality of selected principal aquifer systems. Ground Water 46, 259–271. https://doi.org/10.1111/j.1745-6584.2007.00385.x

Moss, M.E., Kanarek, M.S., Anderson, H.A., Hanrahan, L.P., Remington, P.L., 1995. Osteosarcoma, seasonality, and environmental factors in Wisconsin, 1979–1989. Arch. Environ. Heal. An Int. J. 50, 235–241. https://doi.org/10.1080/00039896.1995.9940393

Mursky, G., Anderson, J.W., Cook, T.R., Meddaugh, W.S., 1989. Uranium and thorium in selected Precambrian rock units in Wisconsin. Geosci. Wisconsin 13.

Nathwani, J.S., Phillips, C.R., 1979. Adsorption of 226Ra by soils in the presence of Ca2+ ions. Specific adsorption (II). Chemosphere 8, 293–299. https://doi.org/10.1016/0045-6535(79)90112-7

Oden, J.H., Szabo, Z., 2016. Arsenic and radionuclide occurrence and relation to geochemistry in groundwater of the Gulf Coast Aquifer System in Houston, Texas, 2007–11, Scientific Investigations Report. https://doi.org/10.3133/sir20155071

Parsen, M.J., Bradbury, K.R., Hunt, R.J., Feinstein, D.T., 2016. The 2016 groundwater flow model for Dane County, Wisconsin, Bulletin.

Reynolds, B.C., Wasserburg, G.J., Baskaran, M., 2003. The transport of U- and Th-series nuclides in sandy confined aquifers. Geochim. Cosmochim. Acta 67, 1955–1972. https://doi.org/10.1016/S0016-7037(02)01341-8

Reynolds, B.C., Wasserburg, G.J., Baskaran, M., 2003. The transport of U- and Th-series nuclides in sandy confined aquifers. Geochim. Cosmochim. Acta 67, 1955–1972. https://doi.org/10.1016/S0016-7037(02)01341-8

Rowe, H., Hughes, N., Geology, K.R.-C., 2012, U., 2012. The quantification and application of handheld energy-dispersive X-ray fluorescence (ED-XRF) in mudrock chemostratigraphy and geochemistry. Elsevier.

Rowland, R.E., Stehney, A.F., Lucas, H.F., 1978. Dose-response relationships for female radium dial workers. Radiat. Res. 76, 368. https://doi.org/10.2307/3574786

Sajih, M., Bryan, N.D., Livens, F.R., Vaughan, D.J., Descostes, M., Phrommavanh, V., Nos, J., Morris, K., 2014. Adsorption of radium and barium on goethite and ferrihydrite: A kinetic and surface complexation modelling study. Geochim. Cosmochim. Acta 146, 150–163. https://doi.org/10.1016/j.gca.2014.10.008

Senior, L., Vogel, K., 1995. Radium and radon in ground water in the Chickies quartzite, southeastern Pennsylvania.

Siegel, D.I., 1990. Sulfur isotope evidence for regional recharge of saline water during continental glaciation, north-central United States. Geology 18, 1054. https://doi.org/10.1130/0091-7613(1990)018<1054:SIEFRR>2.3.CO;2

Stackelberg, P.E., Szabo, Z., Jurgens, B.C., 2018. Radium mobility and the age of groundwater in public-drinking-water supplies from the Cambrian-Ordovician aquifer system, north-central USA. Appl. Geochemistry 89, 34–48. https://doi.org/10.1016/J.APGEOCHEM.2017.11.002

Sturchio, N.C., Banner, J.L., Binz, C.M., Heraty, L.B., Musgrove, M., 2001. Radium geochemistry of ground waters in Paleozoic carbonate aquifers, midcontinent, USA. Appl. Geochemistry 16, 109–122. https://doi.org/10.1016/S0883-2927(00)00014-7

Szabo, Z., dePaul, V.T., Fischer, J.M., Kraemer, T.F., Jacobsen, E., 2012. Occurrence and geochemistry of radium in water from principal drinking-water aquifer systems of the United States. Appl. Geochemistry 27, 729–752. https://doi.org/10.1016/j.apgeochem.2011.11.002

Tomita, J., Satake, H., Fukuyama, T., Sasaki, K., Sakaguchi, A., Yamamoto, M., 2010. Radium geochemistry in Na–Cl type groundwater in Niigata Prefecture, Japan. J. Environ. Radioact. 101, 201–210. https://doi.org/10.1016/J.JENVRAD.2009.10.009

Tricca, A., Porcelli, D., Wasserburg, G.J., 2000. Factors controlling the groundwater transport of U, Th, Ra, and Rn. J. Earth Syst. Sci. 109, 95–108. https://doi.org/10.1007/BF02719153

Tricca, A., Wasserburg, G.J., Porcelli, D., Baskaran, M., 2001. The transport of U-and Th-series nuclides in a sandy unconfined aquifer. Geochim. Cosmochim. Acta 65, 1187–1210.

U.S. Department of the Interior, U.S. Geological Survey, 2012. Prinicipal aquifers can contribute radium to sources of drinking water under certain geochemical conditions. Fact Sheet 2010–3113.

U.S. EPA, 2000. National primary drinking water regulations. Fed. Regist. 65.

Vinson, D.S., Lundy, J.R., Dwyer, G.S., Vengosh, A., 2018. Radium isotope response to aquifer storage and recovery in a sandstone aquifer. Appl. Geochemistry. https://doi.org/10.1016/J.APGEOCHEM.2018.01.006

Vinson, D.S., Lundy, J.R., Dwyer, G.S., Vengosh, A., 2012. Implications of carbonate-like geochemical signatures in a sandstone aquifer: Radium and strontium isotopes in the Cambrian Jordan aquifer (Minnesota, USA). Chem. Geol. 334, 280–294. https://doi.org/10.1016/j.chemgeo.2012.10.030

Vinson, D.S., Tagma, T., Bouchaou, L., Dwyer, G.S., Warner, N.R., Vengosh, A., 2013. Occurrence and mobilization of radium in fresh to saline coastal groundwater inferred from geochemical and isotopic tracers (Sr, S, O, H, Ra, Rn). Appl. Geochemistry 38, 161–175. https://doi.org/10.1016/J.APGEOCHEM.2013.09.004

Vinson, D.S., Vengosh, A., Hirschfeld, D., Dwyer, G.S., 2009. Relationships between radium and radon occurrence and hydrochemistry in fresh groundwater from fractured crystalline rocks, North Carolina (USA). Chem. Geol. 260, 159–171. https://doi.org/10.1016/j.chemgeo.2008.10.022

Weaver, T.R., Bahr, J., 1991a. Geochemical evolution in the Cambrian-Ordovician sandstone aquifer, eastern Wisconsin: 1. Major ion and radionuclide distribution. Ground Water 29, 350–356. https://doi.org/10.1111/j.1745-6584.1991.tb00525.x

Weaver, T.R., Bahr, J.M., 1991b. Geochemical evolution in the Cambrian-Ordovician sandstone aquifer, eastern Wisconsin: 2. Correlation between flow paths and ground-water chemistry.

Ground Water 29, 510–515.

Wilson, J.T., 2012. Water-quality assessment of the Cambrian-Ordovician aquifer system in the Northern Midwest, United States: U.S. Geological Survey, Scientific Investigations Report 2011-5229.

Winter, B.L., Johnson, C.M., Simo, J.A., Valley, J.W., 1996. Paleozoic fluid history of the Michigan Basin: evidence from dolomite geochemistry in the middle Ordovician St. Peter Sandstone. J. Sediment. Res. 65.

Young, H.L., Siegel, D.I., 1992. Hydrogeology of the Cambrian-Ordovician Aquifer System in the Northern Midwest, United States: United States. United States Geol. Surv. Prof. Pap. 1405-B 99.

Zambito, J.J., McLaughlin, P.I., Haas, L.D., Stewart, E.K., Bremmer, S.E., Hurth, M.J., 2016. Sampling methodologies and data analysis techniques for geologic materials using portable X-ray fluorescence (pXRF ) elemental analysis: Wisconsin Geological and Natural History Survey, Open-File Report 2016-02.

## Supporting Information

SI Table 1. Sample field measurements and radium activity results from various sampling seasons. The Minimum Detectable Activity at a 95 % confidence interval is represented by MDA 95. Ports sampled from the Sentry Well are represented as SW.

| Sample ID | Sampling Date | Screen Midpoint (meters below surface) | Screen Length (meters) | Hydrostratigraphic Unit | pH | Temperature (°C) | Specific conductance (µS/cm) | DO (mg/L) | Radium-228 (pCi/L) | Radium-226 (pCi/L) | Combined Radium (pCi/L) |
|---|---|---|---|---|---|---|---|---|---|---|---|
| MW-PL1 | 10/27/16 | * | * | Control | * | * | * | * | 0.7 ± 0.4 | 0.5 ± 0.3 | 1.1 ± 0.5 |
| MW-PL2 | 5/31/17 | * | * | Control | * | * | * | * | < MDA 95 | < MDA 95 | < MDA 95 |
| MW-7S | 10/24/16 | 12 | 5 | Tunnel City | 7.1 | 12.2 | 3030 | ** | 0.7 ± 0.4 | 0.4 ± 0.2 | 1.1 ± 0.4 |
| MW-7S | 5/30/17 | 12 | 5 | Tunnel City | 6.8 | 13.4 | 2390 | 9.1 | < MDA 95 | 0.5 ± 0.3 | 0.9 ± 0.7 |
| MW-11S | 10/21/16 | 13 | 3 | Tunnel City | 7.0 | 11.2 | 2240 | ** | 1.4 ± 0.5 | 0.7 ± 0.3 | 2.1 ± 0.6 |
| MW-11S | 5/25/17 | 13 | 3 | Tunnel City | 6.9 | 12.4 | 2300 | 7.3 | < MDA 95 | 0.5 ± 0.3 | < MDA 95 |
| MW-19S | 10/14/16 | 16 | 5 | Tunnel City | 7.3 | 12.2 | 1390 | ** | < MDA 95 | 0.3 ± 0.2 | 0.6 ± 0.4 |
| MW-19S | 12/11/17 | 16 | 5 | Tunnel City | 6.3 | 12.8 | 1250 | 8.8 | ** | ** | ** |
| MW-30S | 10/14/16 | 19 | 5 | Tunnel City | 7.3 | 10.6 | 920 | ** | < MDA 95 | 0.2 ± 0.1 | < MDA 95 |
| MW-30S | 12/11/17 | 19 | 5 | Tunnel City | 6.8 | 11.3 | 800 | 8.5 | ** | ** | ** |
| MW-13S | 10/24/16 | 16 | 3 | Tunnel City | 7.2 | 11.3 | 1630 | ** | 1.0 ± 0.4 | 0.10 ± 0.07 | 1.1 ± 0.4 |
| MW-13S | 12/11/17 | 16 | 3 | Tunnel City | 6.3 | 11.9 | 1030 | 9.9 | ** | ** | ** |
| SW – port 1 | 10/17/16 | 27 | 1.5 | Tunnel City | 7.3 | 13.0 | 1400 | ** | < MDA 95 | 0.5 ± 0.2 | 0.7 ± 0.5 |
| SW – port 1 | 5/25/17 | 27 | 1.5 | Tunnel City | 7.0 | 11.3 | 1770 | 7.8 | ** | ** | ** |
| FB-11S | 10/14/16 | 31 | 1.5 | Tunnel City | 7.5 | 10.0 | 830 | ** | 0.4 ± 0.4 | 0.2 ± 0.1 | 0.6 ± 0.4 |
| FB-11S | 5/22/17 | 31 | 1.5 | Tunnel City | 7.2 | 11.1 | 1010 | 9.5 | < MDA 95 | < MDA 95 | < MDA 95 |
| MW-13D | 10/24/16 | 34 | 1.5 | Tunnel City | 7.2 | 11.2 | 870 | ** | < MDA 95 | 0.4 ± 0.2 | 0.5 ± 0.4 |
| MW-13D | 12/11/17 | 34 | 1.5 | Tunnel City | 6.3 | 11.5 | 810 | 9.1 | ** | ** | ** |
| MW-30D | 10/14/16 | 41 | 1.5 | Tunnel City | 7.4 | 10.5 | 850 | ** | < MDA 95 | 0.2 ± 0.1 | 1.23 ± 0.52 |
| MW-30D | 5/25/17 | 41 | 1.5 | Tunnel City | 6.9 | 11.2 | 1040 | 8.9 | 0.8 ± 0.5 | 0.4 ± 0.3 | 0.5 ± 0.5 |
| FB-11D | 10/14/16 | 52 | 1.5 | Tunnel City | 7.5 | 10.4 | 570 | ** | 0.7 ± 0.5 | 0.4 ± 0.2 | 1.1 ± 0.5 |
| FB-11D | 12/11/17 | 52 | 1.5 | Tunnel City | 7.1 | 10.7 | 510 | 10.6 | ** | ** | ** |

| | | | | | | | | | | | |
|---|---|---|---|---|---|---|---|---|---|---|---|
| MW-11D | 10/21/16 | 23.5 | 1.5 | Wonewoc | 7.1 | 11.4 | 1290 | ** | 1.7 ± 0.6 | 0.6 ± 0.3 | 2.3 ± 0.7 |
| MW-11D | 5/22/17 | 23.5 | 1.5 | Wonewoc | 7.1 | 12.2 | 1460 | 5.8 | < MDA 95 | < MDA 95 | < MDA 95 |
| MW-7D | 10/24/16 | 29 | 3 | Wonewoc | 7.1 | 11.8 | 2650 | ** | 1.3 ± 0.5 | 0.8 ± 0.3 | 2.1 ± 0.6 |
| MW-7D | 5/30/17 | 29 | 3 | Wonewoc | 6.6 | 13.0 | 2810 | 10.4 | 1.1 ± 0.6 | 1.0 ± 0.4 | 2.1 ± 0.7 |
| MW-19D | 10/14/16 | 42 | 1.5 | Wonewoc | 7.2 | 11.7 | 2410 | ** | 3.6 ± 0.6 | 1.6 ± 0.3 | 5.2 ± 0.6 |
| MW-19D | 5/22/17 | 42 | 1.5 | Wonewoc | 7.0 | 12.3 | 2110 | 10.6 | 3.4 ± 0.6 | 1.8 ± 0.4 | 5.2 ± 0.8 |
| MW-19D | 12/11/17 | 42 | 1.5 | Wonewoc | 6.3 | 12.0 | 1520 | 10.1 | ** | ** | ** |
| SW – port 2 | 10/17/16 | 63 | 1.5 | Wonewoc | 7.3 | 12.6 | 590 | ** | 0.5 ± 0.4 | 0.09 ± 0.08 | 0.6 ± 0.5 |
| SW – port 2 | 5/25/17 | 63 | 1.5 | Wonewoc | 7.2 | 11.3 | 710 | 8.2 | ** | ** | ** |
| MW-7VD | 10/24/16 | 64 | 3 | Wonewoc | 7.3 | 11.0 | 820 | ** | 1.2 ± 0.5 | 0.6 ± 0.3 | 1.8 ± 0.6 |
| MW-7VD | 5/30/17 | 64 | 3 | Wonewoc | 6.9 | 12.1 | 980 | 2.1 | < MDA 95 | 0.3 ± 0.2 | < MDA 95 |
| LE-D | 10/21/16 | 71 | 1.5 | Wonewoc | 7.3 | 10.9 | 620 | ** | < MDA 95 | MDA 95 | < MDA 95 |
| LE-D | 5/30/17 | 71 | 1.5 | Wonewoc | 6.7 | 11.9 | 760 | 2.8 | < MDA 95 | 0.3 ± 0.2 | < MDA 95 |
| SW – port 3 | 5/12/16 | 81.5 | 1.5 | Eau Claire aquitard | 7.3 | 13.5 | 590 | ** | < MDA 95 | < MDA 95 | < MDA 95 |
| SW – port 3 | 5/25/17 | 81.5 | 1.5 | Eau Claire aquitard | 7.2 | 11.4 | 720 | 6.3 | ** | ** | ** |
| SW – port 4 | 10/17/16 | 91 | 1.5 | Mount Simon | 7.4 | 12.3 | 640 | ** | < MDA 95 | 0.4 ± 0.2 | 0.8 ± 0.6 |
| SW – port 4 | 5/25/17 | 91 | 1.5 | Mount Simon | 7.3 | 12 | 760 | 5.5 | < MDA 95 | 0.3 ± 0.2 | < MDA 95 |
| LE-VD | 10/21/16 | 81 | 1.5 | Mount Simon | 7.2 | 10.8 | 700 | ** | 1.0 ± 0.4 | 0.8 ± 0.2 | 1.8 ± 0.5 |
| LE-VD | 5/30/17 | 81 | 1.5 | Mount Simon | 6.6 | 11.9 | 860 | 0.1 | 0.8 ± 0.5 | 0.4 ± 0.2 | 1.2 ± 0.5 |
| SW – port 5 | 10/17/16 | 124 | 6 | Mount Simon | 7.4 | 12.0 | 570 | ** | 1.1 ± 0.4 | 1.0 ± 0.3 | 2.1 ± 0.5 |
| SW – port 5 | 5/25/17 | 124 | 6 | Mount Simon | 7.4 | 11.6 | 770 | 0.2 | 1.0 ± 0.5 | 0.9 ± 0.3 | 1.9 ± 0.6 |
| SW – port 6 | 10/21/16 | 139 | 6 | Mount Simon | 7.7 | 12.0 | 630 | ** | 2.0 ± 0.5 | 1.8 ± 0.4 | 3.8 ± 0.6 |
| SW – port 6 | 5/25/17 | 139 | 6 | Mount Simon | 7.2 | 12.8 | 760 | 0.0 | 2.1 ± 0.5 | 2.5 ± 0.5 | 4.6 ± 0.7 |

*Not applicable  **Samples were not collected for analysis.

SI Table 2. Redox category designation (McMahon and Chapelle, 2008; Stackelberg et al., 2018).

| Redox Process | DO (mg/L) | Mn(II) (mg/L) | Number of Wells |
|---|---|---|---|
| Oxic | ≥ 0.5 | < 0.05 | 18 |
| Suboxic | < 0.5 | < 0.05 | 1 |
| Anoxic | ≤ 0.5 | ≥ 0.05 | 2 |

**S1: Decay chain**

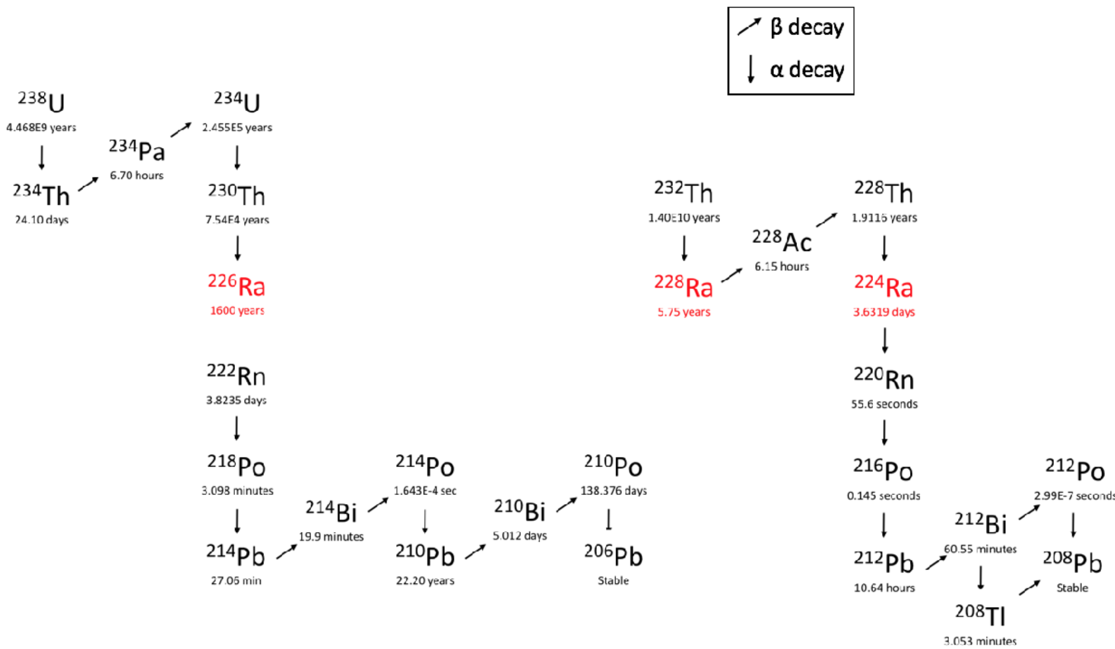


Figure SI-1. Decay chain for radioactive decay of major radium isotope parent nuclides: $^{238}U$ and $^{232}Th$.

## S2: Major ions and trace metal concentrations

Table S1-1. Concentrations of major ions and trace metal parent nuclides from sampled monitoring wells. All values in mg/L unless otherwise noted. Samples below detectable concentration are designated as non-detectable (n.d.).

| Sampling Date | Well | $NO_2^-$ + $NO_3^-$ | $SO_4^{2-}$ | $Cl^-$ | $^{232}$Th (µg/L) | $^{238}$U (µg/L) | Ba | Ca | Mg | Mn | Na |
|---|---|---|---|---|---|---|---|---|---|---|---|
| 10/27/16 | MW-PL1 | 0.0311 | 0.0273 | 0.108 | ** | ** | n.d. | n.d. | n.d. | n.d. | 3.47 ± 0.08 |
| 5/31/17 | MW-PL2 | 0.003 | 0.014 | 0.295 | 0 | 0.000399 ± 0.000008 | n.d. | n.d. | n.d. | n.d. | n.d. |
| 10/24/16 | MW-7S | 1.44 | 79.0 | 662 | ** | ** | 0.0507 ± 0.0006 | 216 ± 2 | 96.1 ± 0.6 | n.d. | 182.8 ± 0.7 |
| 5/30/17 | MW-7S | 5.49 | 49.5 | 435 | 0.005 ± 0.002 | 0.50 ± 0.03 | 0.035 ± 0.002 | 222.6 ± 0.2 | 105.5 ± 0.1 | n.d. | 130.6 ± 0.1 |
| 10/21/16 | MW-11S | 3.96 | 27.5 | 447 | ** | ** | 0.0395 ± 0.0009 | 127 ± 2 | 57.6 ± 0.5 | n.d. | 234 ± 1 |
| 5/25/17 | MW-11S | 4.34 | 31.7 | 444 | 0.0032 ± 0.0003 | 0.36 ± 0.02 | 0.045 ± 0.003 | 168.0 ± 0.8 | 85.2 ± 0.2 | n.d. | 225.2 ± 0.2 |
| 10/14/16 | MW-19S | 3.15 | 25.4 | 238 | ** | ** | 0.0153 ± 0.0002 | 107 ± 2 | 49.5 ± 0. 9 | n.d. | 115 ± 1 |
| 10/14/16 | MW-30S | 7.62 | 28.8 | 42.5 | ** | ** | 0.0077 ± 0.0001 | 107 ± 2 | 49 ± 1 | n.d. | 25.8 ± 0.3 |
| 10/24/16 | MW-13S | 4.38 | 29.5 | 309 | ** | ** | 0.0201 ± 0.0002 | 112 ± 3 | 54 ± 2 | n.d. | 145 ± 3 |
| 10/17/16 | SW - port 1 | 7.00 | 35.6 | 276 | ** | ** | 0.0083 ± 0.0005 | 118 ± 1 | 56.3 ± 0.9 | n.d. | 120.6 ± 0.7 |
| 10/14/16 | FB-11S | 13.5 | 24.4 | 34.5 | ** | ** | 0.0084 ± 0.0003 | 100. ± 0.8 | 46 ± 2 | n.d. | 18.3 ± 0.4 |
| 5/22/17 | FB-11S | 12.6 | 26.6 | 33.3 | 0.0015 ± 0.0003 | 0.3095 ± 0.0009 | n.d. | 120.4 ± 0.7 | 61.8 ± 0.1 | n.d. | 15.0 ± 0.2 |
| 10/24/16 | MW-13D | 5.58 | 22.7 | 49.7 | ** | ** | n.d. | 97 ± 2 | 50. ± 2 | n.d. | 17.4 ± 0.23 |
| 10/14/16 | MW-30D | 6.56 | 15.5 | 33.2 | ** | ** | n.d. | 99 ± 1 | 50.8 ± 0.5 | n.d. | 11.4 ± 0.2 |
| 5/25/17 | MW-30D | 7.42 | 20.9 | 37.3 | 0.0039 ± 0.0004 | 0.52 ± 0.02 | n.d. | 120. ± 0.4 | 70.65 ± 0.05 | n.d. | 9.18 ± 0.05 |
| 10/14/16 | FB-11D | 0.222 | 3.31 | 0.400 | ** | ** | n.d. | 72.7 ± 0.6 | 35.5 ± 0.1 | n.d. | 7.98 ± 0.08 |
| 10/21/16 | MW-11D | 3.88 | 32.4 | 165 | ** | ** | 0.0072 ± 0.0002 | 115 ± 2 | 56.9 ± 0.9 | n.d. | 61.1 ± 0.6 |
| 5/22/17 | MW-11D | 3.55 | 39.5 | 149 | 0.0013 ± 0.0004 | 0.45 ± 0.02 | n.d. | 150.4 ± 0.8 | 80.92 ± 0.07 | n.d. | 45.60 ± 0.08 |
| 10/24/16 | MW-7D | 5.36 | 51.2 | 548 | ** | ** | 0.0231 ± 0.0005 | 165 ± 3 | 78 ± 2 | n.d. | 226 ± 4 |

| | | | | | | | | | | | |
|---|---|---|---|---|---|---|---|---|---|---|---|
| 5/30/17 | MW-7D | 4.98 | 55.6 | 594 | 0.0010 ± 0.0002 | 0.247 ± 0.006 | 0.012 ± 0.002 | 213.7 ± 0.6 | 116.4 ± 0.1 | n.d. | 236.6 ± 0.1 |
| 10/14/16 | MW-19D | 7.39 | 59.2 | 513 | ** | ** | 0.0550 ± 0.0004 | 167 ± 2 | 80. ± 2 | n.d. | 145 ± 2 |
| 5/22/17 | MW-19D | 3.60 | 58.4 | 410. | 0.0013 ± 0.0003 | 0.273 ± 0.005 | 0.065 ± 0.003 | 204.0 ± 0.2 | 105.10 ± 0.09 | n.d. | 131.60 ± 0.07 |
| 10/17/16 | SW - port 2 | 0.543 | 3.18 | 1.54 | ** | ** | n.d. | 72.5 ± 0.9 | 39.1 ± 0.6 | n.d. | 9.1 ± 0.2 |
| 10/24/16 | MW-7VD | 3.23 | 42.1 | 11.7 | ** | ** | 0.0183 ± 0.0004 | 104 ± 3 | 50. ± 2 | 0.0094 ± 0.0002 | 10.2 ± 0.2 |
| 5/30/17 | MW-7VD | 3.47 | 45.0 | 10.6 | 0.0010 ± 0.0003 | 0.57 ± 0.02 | n.d. | 124.9 ± 0.3 | 65.08 ± 0.05 | n.d. | 6.0 ± 0.1 |
| 10/21/16 | LE-D | 1.44 | 14.3 | 5.13 | ** | ** | n.d. | 76 ± 2 | 38 ± 1 | 0.0033 ± 0.0003 | 8.80 ± 0.06 |
| 5/30/17 | LE-D | 1.65 | 20.6 | 5.24 | 0.0010 ± 0.0002 | 0.34 ± 0.02 | n.d. | 90.3 ± 0.2 | 49.91 ± 0.05 | n.d. | 5.4 ± 0.2 |
| 5/12/16 | SW - port 3 | 0.0364 | 4.93 | 0.432 | ** | ** | n.d. | 71 ± 1 | 44.5 ± 0.7 | n.d. | 7.1 ± 0.1 |
| 10/17/16 | SW - port 4 | 3.79 | 19.8 | 11.9 | ** | ** | n.d. | 77 ± 1 | 39 ± 1 | n.d. | 8.7 ± 0.1 |
| 5/25/17 | SW - port 4 | 4.04 | 22.7 | 10.3 | 0.00046 ± 0.00005 | 0.6936 ± 0.0008 | n.d. | 83 ± 0.3 | 50.30 ± 0.07 | n.d. | 5.1 ± 0.09 |
| 10/21/16 | LE-VD | 0.266 | 22.9 | 7.71 | ** | ** | 0.0051 ± 0.0002 | 80 ± 2 | 49.2 ± 0.4 | 0.159 ± 0.002 | 8.6 ± 0.2 |
| 5/30/17 | LE-VD | 0.177 | 23.8 | 8.036 | 0.0032 ± 0.0006 | 5.3 ± 0.1 | n.d. | 93.7 ± 0.3 | 63.79 ± 0.03 | n.d. | 4.8 ± 0.1 |
| 10/17/16 | SW - port 5 | 0.0155 | 3.35 | 0.563 | ** | ** | 0.014 ± 0.001 | 85 ± 1 | 36.0 ± 0.3 | 0.1542 ± 0.0005 | 6.06 ± 0.07 |
| 5/25/17 | SW - port 5 | 0.223 | 4.49 | 0.545 | 0.0008 ± 0.0002 | 0.163 ± 0.004 | n.d. | 93.6 ± 0.2 | 44.15 ± 0.06 | n.d. | 2.34 ± 0.04 |
| 10/21/16 | SW - port 6 | 0 | 18.7 | 2.26 | ** | ** | 0.0120 ± 0.0005 | 76 ± 1 | 41.2 ± 0.5 | 0.0328 ± 0.0008 | 7.32 ± 0.06 |
| 5/25/17 | SW - port 6 | 0.176 | 19.5 | 2.07 | 0.0004 ± 0.0002 | 1.04 ± 0.01 | n.d. | 82.8 ± 0.2 | 52.73 ± 0.05 | n.d. | 3.63 ± 0.04 |

**Samples were not evaluated for analysis.

**S3: Monitoring well tritium values**

Table S1-2. Tritium values for monitoring wells.

| Well | Sampling Date | Tritium (TU) |
|---|---|---|
| FB-11D(Gotkowitz, 2015) | 06/20/12 | 6 ± 2 |
| FB-11S(Gotkowitz, 2015) | 06/20/12 | 10 ± 2 |
| LE-D(Gotkowitz, 2015) | 06/25/12 | < 0.8 ± 2 |
| LE-VD(Gotkowitz, 2015) | 06/25/12 | < 0.8 ± 0.09 |
| MW-11D(Gotkowitz, 2015) | 06/27/12 | 10 ± 2 |
| MW-11S(Gotkowitz, 2015) | 06/27/12 | 4 ± 2 |
| MW-13D(Gotkowitz, 2015) | 06/21/12 | 11 ± 2 |
| MW-13S(Gotkowitz, 2015) | 06/21/12 | 8 ± 2 |
| MW-19D(Gotkowitz, 2015) | 06/18/12 | 10 ± 2 |
| MW-19S(Gotkowitz, 2015) | 06/18/12 | 7 ± 2 |
| MW-30D(Gotkowitz, 2015) | 06/19/12 | < 0.8 ± 2 |
| MW-30S(Gotkowitz, 2015) | 06/19/12 | 7 ± 2 |
| MW-7D(Gotkowitz, 2015) | 06/26/12 | 7 ± 3 |
| MW-7S(Gotkowitz, 2015) | 06/26/12 | 9 ± 2 |
| MW-7VD(Gotkowitz, 2015) | 06/26/12 | < 0.8 ± 2 |
| SW – port 1 | 4/28/14 | 6 ± 0.7 |
| SW – port 2 | 4/28/14 | < 0.8 ± 0.6 |
| SW – port 3 | 4/28/14 | < 0.8 ± 0.5 |
| SW – port 4 | 4/28/14 | 5.3 ± 0.6 |
| SW – port 5 | 4/28/14 | < 0.8 ± 0.5 |
| SW – port 6 | 4/28/14 | < 0.8 ± 0.5 |

**S4: Estimated barite activity calculations**(Brezonik et al., 2011; Ponnamperuma et al., 1966)

Barite activities for each groundwater sample are calculated from measured specific conductance values according to:

$$A_i = \gamma_{\pm 2} C_i \qquad \textbf{S1}$$

where $A_i$ is the activity of the $i$th ion, $\gamma_{\pm 2}$ is the activity coefficient for divalent cations or anions, and $C_i$ is the measured concentration of the $i$th ion. The activity coefficient is calculated via the extended form of the Debye-Hückel equation:

$$\log \gamma_{\pm 2} = -A z_i^2 \left( \frac{\sqrt{I}}{1 + B a_i \sqrt{I}} \right) \qquad \textbf{S2}$$

where $A$ and $B$ are tabulated Debye-Hückel constants (A = 0.511, B = 0.329x$10^8$ for water at 25°C), $z_i^2$ represents the charge value of the $i$th ion, and $a_i$ is the ion size parameter ($a_{barium}$ = 5x$10^{-8}$ cm, $a_{sulfate}$ = 4x$10^{-8}$ cm).(Brezonik et al., 2011) Ionic strength is estimated from the following relationship to measured specific conductance:

$$\mathrm{I} \cong (1.6\mathrm{x}10^{-5})(\text{Specific Conductance}) \qquad \textbf{S3}$$

where I is the ionic strength of the sample.

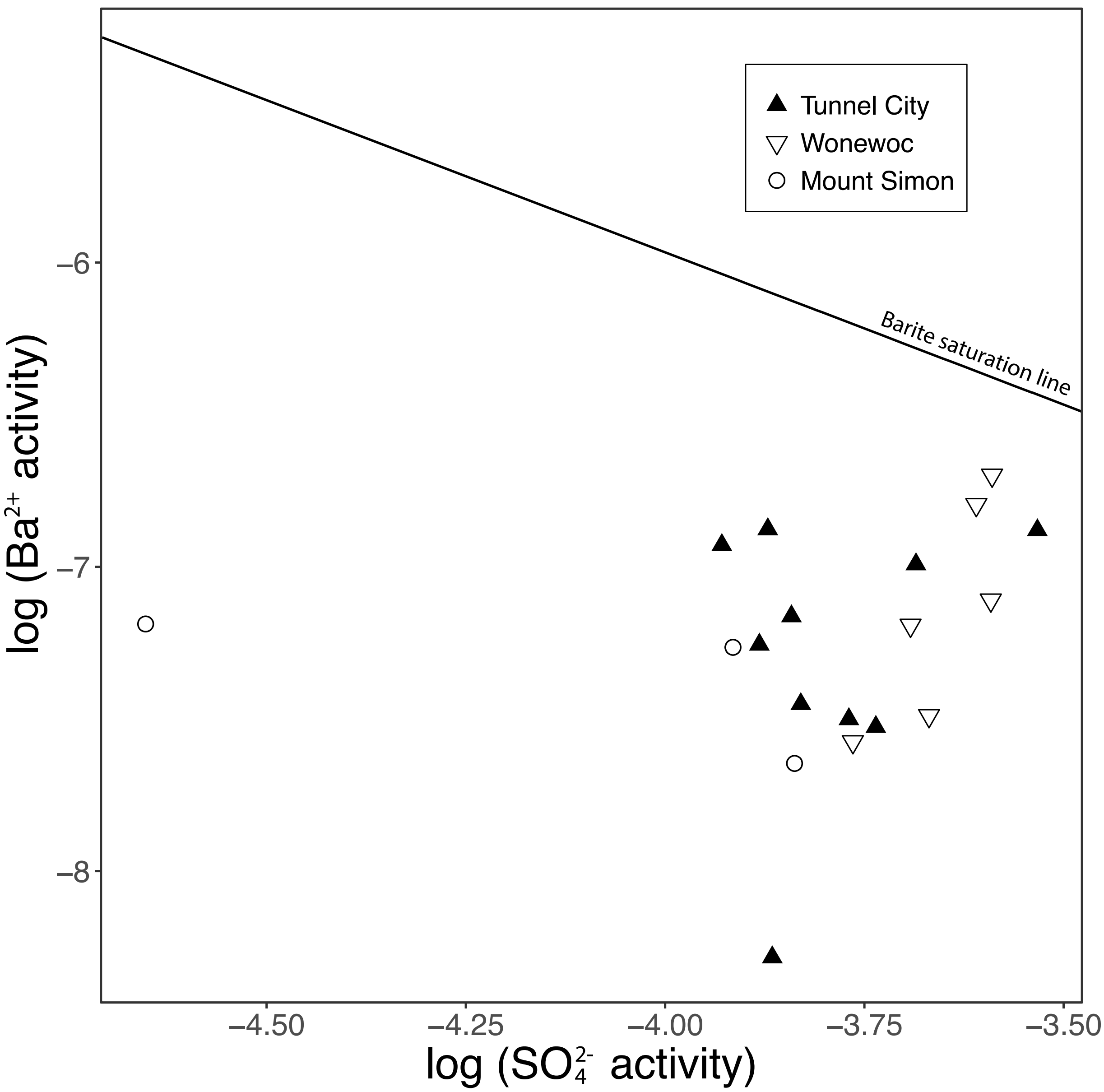

Figure S1-2. Barium activity as a function of sulfate activity from samples above the detection level in both sampling sessions.

## SI References


Brezonik, Patrick L, Arnold, William A, 2011. Water Chemistry.

Gotkowitz, M.B., 2015. Evaluating remedies for pathogen contamination of urban groundwater.

Ponnamperuma, F.N., Tianco, E.M., Loy, T.A., 1966. Ionic strength of the solutions of flooded soils and other natural aqueous solutions from specific conductance. Soil Sci. 102, 408–413.